Dynamic Model of Multi-Species Segregation and Dispersion in Liquid Fluidized Beds

W. Fred Ramirez
Dept. of Chemical and Biological Engineering, University of Colorado, Boulder, CO 80309

K. P. Galvin
School of Engineering, University of Newcastle, NSW 2308, Australia

DOI 10.1002/aic.10457
Published online May 10, 2005 in Wiley InterScience (www.interscience.wiley.com).

Keywords: fluidization, mathematical modeling

Introduction

Liquid-fluidized beds are being used increasingly in a wide range of industries (Di Felice, 1995). Although there has been growing interest in the emerging area of expanded bed adsorption, liquid-fluidized beds are also gaining increasing interest from more traditional areas, such as mineral processing, as evident from the new range of separators; for example, the Knelson concentrator (Rubiera et al., 1997), and the reflux classifier (Galvin, 2003). In these applications the system involves particles covering a wide range of sizes and densities, a significant complication from both a practical and theoretical perspective. More recently, the liquid fluidized bed has been used to obtain the washability curve for a coal and mineral matter feed (that is, the density distribution of the particles), as a replacement for the traditional sink-float method which relies on toxic heavy organic liquids (Galvin, 2003). In this method, particle species that reside at a common position within the liquid-fluidized bed, such as small high density and large low density particles, are sampled and further fractionated by using sieves. The level of segregation achieved in the fluidized bed is clearly dependent upon the particle slip velocities and the levels of dispersion, both of which are poorly understood, especially when the particle size and density varies widely. Our basic objective in this article is to provide a generalized framework for describing the segregation and dispersion of more than two-particle species in a liquid-fluidized bed. While this work is immediately applicable to understanding the limitations of the new washability method, it is also relevant to describing liquid-fluidized beds in general, and to the longer term understanding of the factors that influence the particle slip velocity and dispersion coefficient.

Although the phenomenon of dispersion in liquid-fluidized beds is well recognized, remarkably little work has appeared on the modeling of such systems. Kennedy and Bretton (1966) introduced the concept of a segregation velocity to account for the effects of dispersion on the distribution of particles in a liquid-fluidized bed. Their basic formulation continues to underpin all models referred to in this article including the one we propose. Van Duijn and Rietema (1982) also discuss the phenomena of segregation in liquid-fluidized beds, and Jean and Fan (1986) provide a simple and novel criteria for determining the segregation velocity and, hence, the dispersion, especially in the context of bed inversion. Asif and Petersen (1993) developed a useful analytical solution to describe the concentration distribution, due to the dispersion of a binary system of particles, with a number of restrictions imposed. More recently, Chen et al. (2001, 2002) developed a comprehensive model to describe the segregation and dispersion in a liquid-fluidized bed classifier operated under continuous conditions. Their model used an iterative technique based on the overall material balance to obtain convergence and agreement with the outlet condition.

A common weakness associated with previous models has been the need to know *a priori* the final boundary conditions for the batch fluidized bed, or exit boundary conditions in the case of a fluidized bed operated under continuous conditions. The difficulty of specifying the upper boundary condition in a batch system, especially the variable bed height, is noted in the review by Di Felice (1995). Patwardhan and Chi Tien (1984) used an iterative scheme in conjunction with a mass balance in order to arrive at the steady state concentration profiles. Gibilaro et al. (1985) removed the dependence on height altogether in order to overcome the problem of the boundary condition.

Correspondence concerning this article should be addressed to W. F. Ramirez at fred.ramirez@colorado.edu.

In this article, we detail the complete formulation of a generalized dynamic model of the segregation and dispersion of multiple particle species in a liquid-fluidized bed. We provide a system of first-order differential equations to describe the transport of particles between adjacent layers. Our approach is unique as it does not require knowledge *a priori* of the final boundary conditions. Hence, it is truly predictive, assuming the dispersion coefficient is known. The moving boundary value problem, which arises because of the natural variation of the bed height with time, is transformed into a fixed boundary problem via the front fixing technique of Landau (1950), previously employed by Thelen and Ramirez (1999), to describe the fluidization of a single particle species system.

For illustrative purposes, the steady state predictions of the model are assessed using existing experimental data on a binary system of particles of the same size and slightly different density, and a brief discussion of the predicted dynamics provided. The discussion is then extended to cover the dynamic predictions of a three particle species system.

Theory

In the following analysis the upwards direction is taken as positive. Prior to achieving the final equilibrium state, a given particle species at a specific elevation in the vessel will exhibit a net particle flux relative to the vessel, given by

$$N_i^V = \phi_i v_{p_i} \tag{1}$$

where i represents a single particle species having a specific size and density, v_{p_i} the particle velocity relative to the vessel, and ϕ_i, the local volume fraction of the species concerned. Introducing the usual representations for dispersion and segregation, the following governing equation is obtained. That is

$$N_i^V = \phi_i v_{p_i} = -D_i \frac{\partial \phi_i}{\partial z} + \phi_i v_{s_i} \tag{2}$$

The dispersion of species i is given by the product of the species dispersion coefficient, D_i, and the species concentration gradient $\partial \phi_i / \partial z$. The segregation flux, which is equivalent to the particle flux in the absence of dispersion, is the product of the segregation velocity v_{s_i}, and the local volume fraction of solids ϕ_i. The segregation velocity v_{s_i}, is obtained using

$$v_{s_i} = v_{slip_i} + v_f \tag{3}$$

where v_{slip_i} is the slip velocity of particle species i, and v_f the interstitial fluid velocity. Slip velocities are calculated from a specific phenomenological relation. One model is the traditional Richardson and Zaki (1954) relationship

$$v_{slip_i} = v_{t_i}(1 - \phi)^{n_i - 1} \tag{4}$$

where v_{t_i} is the terminal velocity of the particle species in isolation, ϕ the total volume fraction of all the species at the given location, and n_i an empirical exponent. It is evident from Eq. 2 that when the system reaches equilibrium, and, hence, N_i^V is zero, there exists a direct balance between the dispersion and segregation fluxes. If there is no concentration gradient at steady state, then the segregation velocity must also be zero. However, in the presence of a concentration gradient at steady state, there exists a nonzero segregation velocity. This finite velocity opposes the dispersion, and, hence, is responsible for driving the particles into the segregated state.

In developing the model, the first step involves calculating the interstitial fluid velocity, v_f, which in turn permits the calculation of the segregation velocity via Eq. 3. Continuity requires that the total volume flux through the system equals the superficial fluidization velocity. That is

$$v_f \phi_f + \sum v_{p_i} \phi_i = v_o \tag{5}$$

where ϕ_f is the volume fraction of the fluid, and ϕ_i the volume fraction of species i. The fluid velocity is then obtained by incorporating Eqs. 2 and 3 and rearranging. That is

$$v_f = v_o - \sum \left(-D_i \frac{\partial \phi_i}{\partial z} + v_{slip_i} \phi_i \right) \tag{6}$$

The interstitial fluid velocity is clearly a consequence of the superficial fluidization velocity, and the combined effects of the segregating and dispersing solids. At steady state, the particle flux in Eq. 5 is zero, and, hence, a simpler result for the interstitial fluid velocity can be obtained. That is

$$v_f = v_o / \phi_f \tag{7}$$

Equation 7 is sufficiently accurate under dynamic conditions and, of course, exact as the system reaches steady state. It is noted the fluid volume fraction can be related to the total volume fraction of solids ϕ by $\phi_f = 1 - \phi$, where $\phi = \Sigma \phi_i$.

We now begin the main specification of the model. The dynamic material balance of species i gives

$$\frac{\partial \phi_i}{\partial t} = -\frac{\partial N_i^V}{\partial z} \tag{8}$$

Substituting Eq. 2 into Eq. 8 gives a second-order partial-differential equation

$$\frac{\partial \phi_i}{\partial t} = D_i \frac{\partial^2 \phi_i}{\partial z^2} + \frac{\partial \phi_i v_{s_i}}{\partial z} \tag{9}$$

It has been observed experimentally that, depending upon the initial conditions, some rather significant variations can be experienced in the bed height h. At the top of the bed the flux of species j, the slowest settling species, determines the change in the bed height.

Returning to Eq. 2, and noting that $v_{p_j} = dh/dt$, then

$$\phi_j \frac{dh}{dt} = -D_j \frac{\partial \phi_j}{\partial z} + \phi_j v_{s_j} \tag{10}$$

This variation in the bed height needs to be addressed when introducing finite difference equations to describe the flux transport at each level. Thus, we introduce the dimensionless variable for distance, $z^* = z/h$ to transform the spatial derivatives (Thelen and Ramirez, 1999). The equation for species i, therefore, becomes

$$\frac{\partial \phi_i}{\partial t} = \frac{D_i}{h^2}\frac{\partial^2 \phi_i}{\partial z^{*2}} - \frac{v_{s_i}}{h}\frac{\partial \phi_i}{\partial z^*} - \frac{\phi_i}{h}\frac{\partial v_{s_i}}{\partial z^*} + \frac{z^*}{h}\frac{dh}{dt}\frac{\partial \phi_i}{\partial z^*} \quad (11)$$

The bed height is given by the differential equation at $z^* = 1$ as

$$\frac{dh}{dt} = v_{s_j} - \frac{D_j}{\phi_j h}\frac{\partial \phi_j}{\partial z^*} \quad (12)$$

Here, the volume fraction and segregation velocity used are based on the species that determines the actual bed height, since it is the one that has the lowest slip velocity.

As already noted, we use the earlier dynamic model to approach the steady state solution. The fluidized bed is assumed to have a uniform distribution of particles at time zero. We make a quasi-steady state assumption that the fluid phase dynamics are faster than the particle-phase dynamics. This allows us to use Eq. 7 rather than Eq. 6.

Solution Strategy

The solution strategy adopted to solve the mathematical model was based on the method of lines (Crank, 1984). Due to the nonlinearities in the model, finding stable finite difference schemes can be difficult. Since the method of lines only uses finite differences for the distance derivatives, the solution can be obtained using a system of ordinary differential equations with sufficiently small time intervals. However, by using a very robust ordinary differential equation solver for the time domain, the size of the time interval can be expanded, while ensuring stability. For this problem a stiff differential equation solver is required due to the very nonuniform dynamic behavior of the system. The stiff differential equation routine ode15s of Matlab® (Matlab is a trade mark of MathWorks, Inc.) was used. The set of ordinary differential equations become

$$\frac{d\phi(i)_k}{dt} = \frac{D(i)}{h^2\Delta z^{*2}}\left(\phi(i)_{k+1} - 2\phi(i)_k + \phi(i)_{k-1}\right) - \frac{v_s(i)_k}{2h\Delta z^*}\left(\phi(k)_{k+1} - \phi(k)_{k-1}\right) - \frac{\phi(i)_k}{h\Delta z^*}\left(v_s(i)_{k+1} - v_s(i)_k\right) + \frac{z_k^*}{2h\Delta z^*}\frac{dh}{dt}\left(\phi(i)_{k+1} - \phi(i)_{k-1}\right) \quad (13)$$

where k indicates the spatial location.

The no flux boundary condition at the bottom of the bed, $z^* = 0$, is

$$\phi(i)_0 = \phi(i)_2 - \frac{2v_s(i)_1 h\Delta z^*}{D(i)}\phi(i)_1 \quad (14)$$

Table 1. Monocomponent Data for Particles Species used in the Binary Experiments

Particle Density (kg/m^3)	Richardson-Zaki Exponent n	Terminal Velocity (m/s)
1,300	2.8	0.053
1,400	2.9	0.059

At the top of the bed, $z^* = 1$, the no flux boundary condition applies to all species since they do not leave the fluidized bed. This condition still permits an expansion in the actual bed height, however

$$\phi(i)_{H+1} = \phi(i)_{H-1} + \frac{2v_s(i)_H h\Delta z^*}{D(i)}\phi(i)_H \quad (15)$$

The finite differencing for the bed height relation becomes

$$\frac{dh}{dt} = v_s(j)_H - \frac{D(j)}{\phi(j)_H h\Delta z^*}\left(\phi(j)_H - \phi(j)_{H-1}\right) \quad (16)$$

Assessment of the Dynamic Model

Recently, Callen et al. (2002) demonstrated and quantified the phenomenon of dispersion using a model particle system consisting of just two species under batch conditions. The particle species were of the same nominal size, ranging from 1.18 to 1.40 mm, however, one was 1400 kg/m^3, and the other 1300 kg/m^3 in density. The sedimentation behavior of each species was characterised experimentally on its own using the Richardson and Zaki (1954) equation, to obtain the empirical terminal velocities and exponents needed in Eq. 4. The values are provided in Table 1.

The numerical results in Figures 1a and 1b, show the complex transient nature of the dispersion phenomenon, and, also, the final steady-state solution for the heavier and lighter species, respectively. Figure 2 shows the theoretical bed height progression, with an initial rise, a contraction, and then an approach towards the equilibrium value of about 1.26 meters. It is evident that the final bed height is predicted rather than imposed. The numerical solution was based on an initial uniform concentration distribution for each species. In the absence of a satisfactory model for predicting the dispersion coefficient, the Peclet number was adjusted in order to produce the best possible agreement between the steady state solution and the experimental data. Although a common dispersion coefficient was used for the two species, because of their similar size and density, each species can in principle be prescribed a different value. At the superficial fluidization velocity of 0.045 m/s, the final bed height was 1.26 m, the dispersion coefficient 0.0006 m^2/s, and, hence, the Peclet number $v_o h/D$, 95. The calculated steady-state conditions provide a reasonable fit of the experimental data.

The dynamic behavior of the heavier species shown in Figure 1a indicates a relatively uniform approach toward steady state. The dynamic response of the lighter species shown in Figure 1b, however, indicates a very nonuniform response at the top of the bed. It is very interesting to note that the volume fraction of the lighter species, which eventually reaches a maximum at the top of the bed, passes through a time

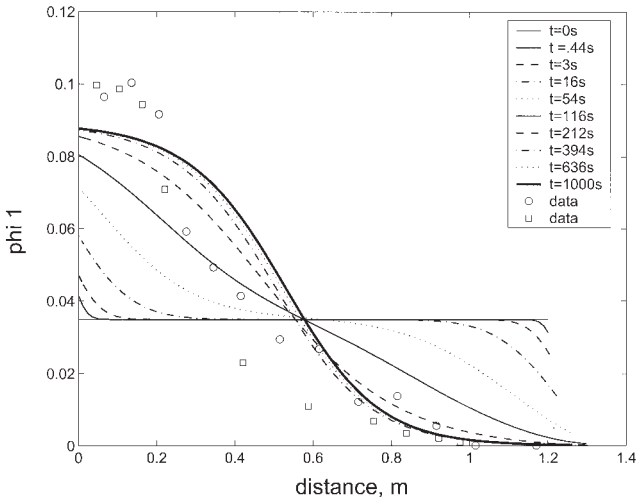

Figure 1a. Concentration distribution for heavier species.

Superficial fluidization velocity = 0.045 m/s. Dispersion coefficient = 0.0006 m^2/s. Model predicts the progression toward steady state with the time values indicated. Experimental data are indicated by the discrete points (circles are used to denote data based on the pressure transducer readings, square symbols used to denote data obtained by manual separation of the particles).

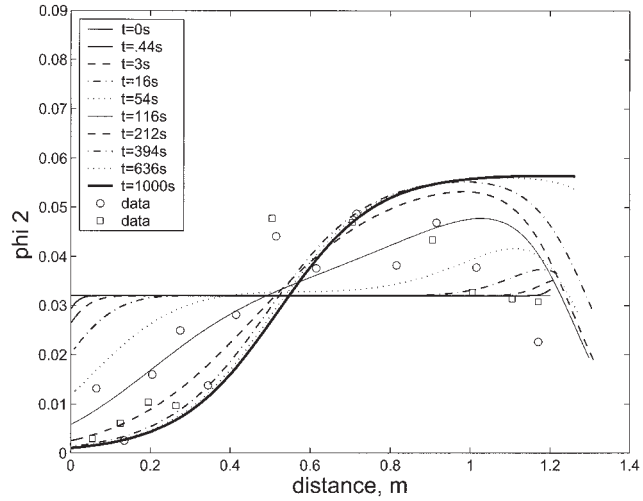

Figure 1b. Concentration distribution for lighter species.

Superficial fluidization velocity = 0.045 m/s. Dispersion coefficient = 0.0006 m^2/s. Model predicts the progression toward steady state with the time values indicated. Experimental data are indicated by the discrete points (circles are used to denote data based on the pressure transducer readings, square symbols used to denote data obtained by manual separation of the particles).

period when the value is lower than the initial uniform value (times of 116, 212, and 394 s). There is then a dramatic rise in the volume fraction value at the top of the bed during the time period of 394 to 636 s, and then a uniform approach toward the steady state condition. The experimental data in Figure 1b near the top of the bed exhibit a decreasing volume fraction, similar to that obtained numerically prior to the final steady state. This finding suggests that the data reported by Callen et al. (2002) may have been obtained before the actual steady state was reached. The theoretical time required for the lighter species concentration to reach the equilibrium value near the top of the bed was about 15 min.

It is noted that the solution can sometimes become unstable near the top of the bed due to the rate of change in the bed height being dependent on the term $(D_j/h\phi_j)(\partial\phi_j/\partial z)$, as shown in Eq. 13. This term could become singular if the volume fraction of the lighter species at the top of the bed decreased toward zero more rapidly than the concentration gradient term. If the dispersion coefficient is marginally too large, the overall term exceeds the maximum possible segregation velocity in Eq. 12, and, hence, the bed height grows without limit. It is noted, however, that this growth is associated with an infinitesimal concentration of the lighter species, and that the effective bed height still remains finite. A slight reduction in the value of the dispersion coefficient of the lighter species at the top of the bed is generally enough to overcome this effect.

Figure 3 shows the theoretical concentration distributions for a three species system, based on the circumstances of the experiment run at a superficial fluidization velocity of 0.045 m/s, and a dispersion coefficient for each species of 0.0006 m^2/s. Again, a common dispersion coefficient has been chosen for convenience, given the particles are so similar in size and density. For this simulation, the terminal velocity of the third species was set at 0.056 m/s, and the Richardson and Zaki exponent at 2.8. This result is presented in order to demonstrate the generality of the model developed in this study for any number of species. It is evident that the three particle species overlap considerably and, hence, that there is a loss of the monocomponent presence evident in the previous cases. A considerable period of time was required to achieve satisfactory convergence of the solution, involving some subtle evolution in the concentration distributions in order to produce the correct steady state segregation velocity distributions. The dynamic response of the heavier species shown in Figure 3a is

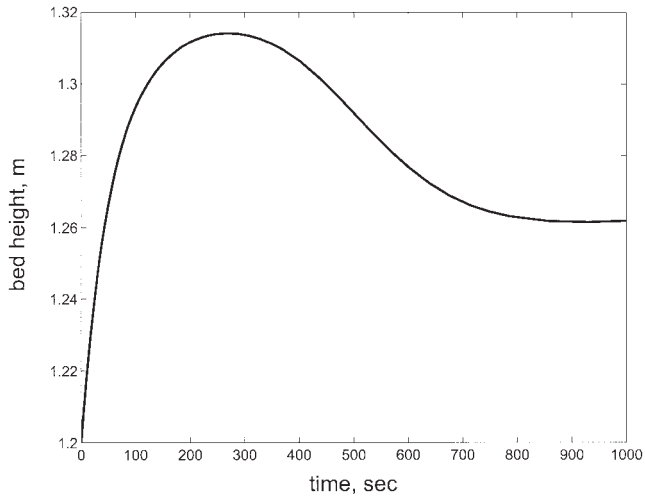

Figure 2. Variation in bed height vs. time for the experiment conducted at a superficial fluidization velocity of 0.045 m/s, showing convergence to the final steady-state bed height of 1.26 m.

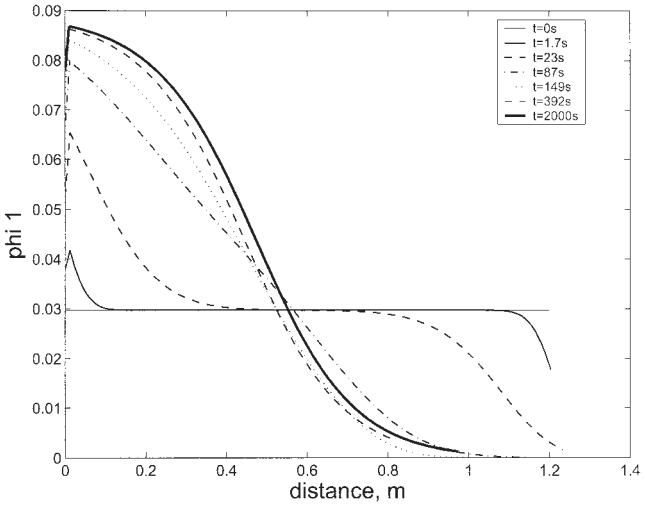

Figure 3a. Concentration distribution for the heaviest species in a three species system. Superficial velocity = 0.045 m/s.

The dispersion coefficient = 0.0006 m^2/s. The model predicts the progression towards steady state with the time values indicated.

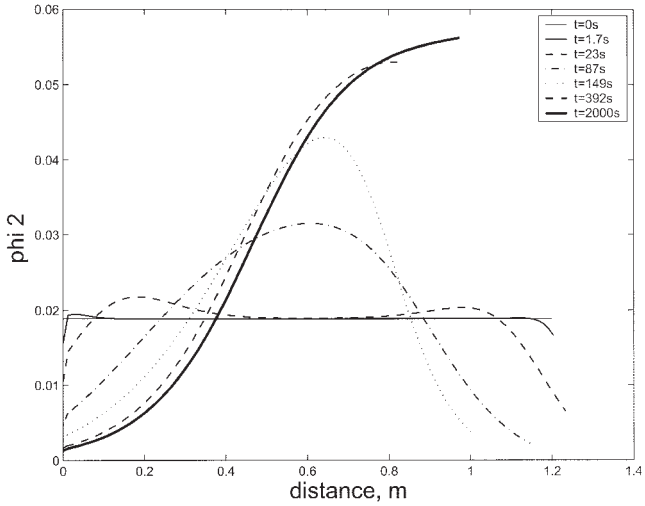

Figure 3c. Concentration distribution for the lightest species in a three species system. Superficial velocity = 0.045 m/s.

The dispersion coefficient = 0.0006 m^2/s. The model predicts the progression toward steady state with the time values indicated.

similar to that for the binary case. Although, the steady-state distribution for the lighter species is similar to that for the binary case, the dynamics is quite different as shown in Figure 3c. The distribution at early times shows low volume fractions at both the top and bottom of the bed with bimodal maximums (times 0.34 through to 51 s). A single maximum then develops and the top volume fraction starts to increase (times 92 though to 415 s). Finally, the maximum disappears and the final shape of the distribution develops (times 832 and 1,500 seconds). The final distribution for the middle species shows a maximum in the central part of the bed as shown in Figure 3b. The distributions at earlier times for the middle species is very similar to that of the light species, however, the bottom volume fractions are larger and only a single maximum exists at all times for the middle species. It is interesting to note that at steady state the middle species exists over the entire domain of the bed, although with higher concentrations near the middle of the bed.

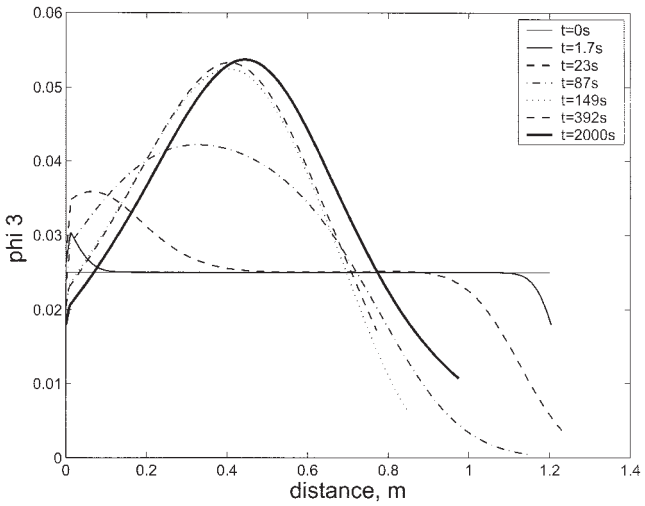

Figure 3b. Concentration distribution for the middle species in a three species system.

Superficial velocity = 0.045 m/s. The dispersion coefficient = 0.0006 m^2/s. The model predicts the progression toward steady state with the time values indicated.

Conclusions

A mathematical model of a liquid-fluidized bed was derived using a dynamic flux balance of the particle segregation and dispersion. Unlike previous models, this model relies only on the initial conditions, with the final steady-state distribution of the particle species arrived at dynamically. The solution yields the concentration distribution of each species, the bed height, as well as the corresponding segregation velocities. The steady-state concentration distributions of the species obtained using the model were in good agreement with the corresponding experimental data, once the optimum axial dispersion coefficient was used. The dynamics of the process show very non-uniform behavior and, hence, special numerical methods are required to solve the dynamic model.

Acknowledgments

Research for this project was supported in part by the Council on Research and Creative Work at the University of Colorado at Boulder, USA, and the University of Newcastle, Australia.

Literature Cited

Asif, M., and J. N. Peterson, Particle Dispersion in a Binary Solid-Liquid Fluidised Bed, *AIChE J.,* **39(9)**, 1465–1471 (1993).

Callen, A. M., S. J. Pratten, N. Lambert, and K. P. Galvin, *Measurement of the Density Distribution of a System of Particles using Water Fluidization,* World Congress on Particle Technology 4, Sydney (2002).

Chen, A., J. R. Grace, N. Epstein, and C. J. Lim, Steady State Hydrodynamic Model for Continuous Particle Classification in a Liquid Fluidized

Bed. In: M. Kwauk, J. Li, and W. C. Yang (Eds.), Fluidization X, 413–420, New York, United Engineering Foundation (2001).
Chen, A., J. R. Grace, N. Epstein, and C. J. Lim, "Steady State Dispersion of Mono-Size, Binary and Multi-Size Particles in a Liquid Fluidized Bed Classifier," *Chem. Eng. Sci.,* **57**(6), 991–1002 (2002).
Crank, J., Free and Moving Boundary Problems, Clarendon Press, Oxford (1984).
Di Felice, R., "The voidage function for Fluid-Particle Interaction Systems," *Int. J. of Multiphase Flow,* **20**, 153–159 (1994).
Di Felice, R., "Hydrodynamics of Liquid Fluidisation," *Chem. Eng. Sci.,* **50**(8), 1213–1245 (1995).
Galvin, K. P., On the Phenomena of Hindered Settling in Liquid Fluidized Beds, in Advances in Gravity Concentration, Edited by R. Q. Honaker and W. R. Forrest, Published by SME, 19–38 (2003).
Gibilaro, L. G., I. Hossain, and S. P. Waldram, "On the Kennedy and Bretton Model for Mixing and Segregation in Liquid Fluidized Beds," *Chem. Eng. Sci.* **40**, 2333–2338 (1985).
Kennedy, S. C., and J. F. Bretton, "Axial Dispersion of Spheres Fluidized with Liquids," *AIChE J.* **12**, 24–30 (1966).
Landau, H. G., *Q. Appl. Math.,* **8**, 81 (1950).
Patwardhan, V. S., and C. Tien, "Distribution of Solid Particles in Liquid Fluidized Beds," *Can. J. of Chem. Eng.* **62**, 46–54 (1984).
Richardson, J. F., and W. N. Zaki, "Sedimentation and Fluidization: Part I," *Trans. Inst. Chem. Eng.,* **32**, 35 (1954).
Rubiera, F., S. T. Hall, and C. L. Shah, "Sulfur Removal by Fine Coal Cleaning Processes," *Fuel,* **76**(13), 1187–1194 (1997).
Thelen, T. V., and W. F. Ramirez, "Modeling of Solid-Liquid Fluidization in the Stokes Flow Regime Using Two-Phase Flow Theory," *AIChE J.* **45**, 708–723 (1999).
van Duijn, G., and K. Rietema, "Segregation of Liquid-Fluidized Solids," *Chem. Eng. Sci.,* 37(5), 727–733 (1982).

Manuscript received Apr. 15, 2004, and revision received Nov. 5, 2004.